THE JOURNAL OF PHYSICAL CHEMISTRY B

Article

pubs.acs.org/JPCB

Impact of Vibrational Entropy on the Stability of Unsolvated Peptide Helices with Increasing Length

Mariana Rossi,* Matthias Scheffler, and Volker Blum

Fritz-Haber-Institut der Max-Planck-Gesellschaft, Faradayweg 4-6, 14195 Berlin, Germany

Supporting Information

ABSTRACT: Helices are a key folding motif in protein structure. The question of which factors determine helix stability for a given polypeptide or protein is an ongoing challenge. Here we use van-der-Waals-corrected density functional theory to address a part of this question in a bottom-up approach. We show how intrinsic helical structure is stabilized with length and temperature for a series of experimentally well-studied unsolvated alanine-based polypeptides, Ac-Ala$_n$-LysH$^+$. By exhaustively exploring the conformational space of these molecules, we find that helices emerge as the preferred structure in the length range n = 4−8 not just due to enthalpic factors (hydrogen bonds and their cooperativity, van der Waals dispersion interactions, electrostatics) but importantly also by a vibrational entropic stabilization over competing conformers at room temperature. The stabilization is shown to be due to softer low-frequency vibrational modes in helical conformers than in more compact ones. This observation is corroborated by including anharmonic effects explicitly through *ab initio* molecular dynamics and generalized by testing different terminations and considering larger helical peptide models.

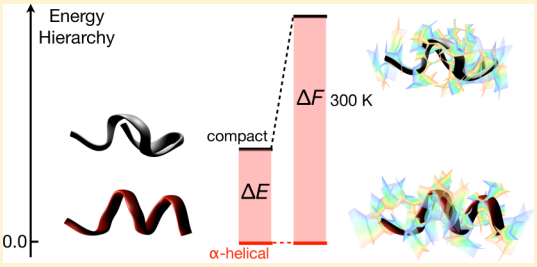

INTRODUCTION

Polypeptide helices are a key secondary structure motif in a wide range of polypeptides and proteins.[1−3] It is well known that some amino acids (e.g., alanine) exhibit a stronger helix propensity than others,[4−11] but the fact that the helical structure is so abundant[12,13] in peptides and proteins is still intriguing. Helices appear in many of the most important proteins[14−16] and are also an important ingredient in protein design (e.g., refs 13, 17, and 18). The ability to quantify the competition of peptide helices with other possible structure elements is thus critical for properties related to biology and also to rather nonbiological chemistry, such as enzyme catalysis in organic solvents,[19,20] at solid surfaces,[21] or in thin films[22] or peptide-driven synthesis of nanoparticles.[23,24]

From a thermodynamic point of view, there are at least two possible limits in which helices compete with other structure prototypes. Toward high temperature, one expects the transition to a random coil,[25] which should become entropically favored as the temperature increases. Toward low temperature, however, helices may themselves compete with other enthalpically stable conformations. In fact, in the most interesting regime, namely, at ambient temperatures, stability may be determined by a delicate balance between enthalpy and entropy.[26] Using density functional theory (DFT) including van der Waals (vdW) dispersion interactions,[27] we here unravel this balance quantitatively for the emergence of helical structure in a particularly well-studied series of unsolvated polyalanine-based peptides Ac-Ala$_n$-LysH$^+$, n = 4−8.[28−31] We consider explicitly not just the helical part of conformational space but actually the much larger, general low-energy conformational space of the peptides, of which helices are a part. We show from first principles: (i) a comprehensive search of the conformational space for Ac-Ala$_n$-LysH$^+$, n = 4−8, involving thousands of possible conformers; (ii) harmonic free-energy calculations for a broad range of the most favorable structural candidates; (iii) the role of anharmonicities in the potential energy surface (PES); and (iv) a theoretical comparison to longer model peptides with a different termination, considering only helical motifs, to clarify the impact of Lys on the soft vibrational modes. Our work is based on an exhaustive prediction of low-energy conformers using DFT and the PBE[32] exchange-correlation functional, corrected to account for long-range vdW interactions[27] (here called PBE+vdW). This level of theory treats accurately, and without system-specific empirical parameters, critical length-dependent contributions such as H-bond cooperativity[31,33−36] and vdW dispersion interactions,[31] including their effect on vibrational frequencies and in *ab initio* molecular dynamics. Our key finding is that there is a significant vibrational entropic stabilization of helices compared with other, more compact conformers, a contribution that should indeed make a difference in actual proteins as well. This contribution is intrinsic to the helix and should therefore act largely independently, not entangled with environment-dependent terms such as a solvent entropy.

Terms That Shape the Potential Energy Surface of Polypeptide Helices. Beginning with the terms that shape the PES, known reasons for helix stability include[37,38] (i) their efficient hydrogen-bond (H-bond) network and increasing H-

Received: February 28, 2013
Revised: April 8, 2013
Published: April 9, 2013

   dx.doi.org/10.1021/jp402087e | J. Phys. Chem. B 2013, 117, 5574−5584

bond cooperativity with helix length,[31,33−36] (ii) suitably bonded and/or electrostatically favorable termination, for instance, the $LysH^+$ termination considered here,[39−45] and (iii) remarkably, a rather specific favorable contribution of vdW dispersion interactions for α-helices.[31,46] Clearly, the peptide chain length plays a role: Too short chains have too few and too weak hydrogen bonds for helices to compensate for the cost of strain in the backbone.[29,43,47−49] In practice, environment effects will necessarily influence helix stability.[49−52] In an aqueous medium, the hydrophobic effect will be prominent,[53] but it is important to note that peptides and proteins are also found (and used) in different environments. In water-poor conditions, like membranes, helices are frequently observed.[54,55] Understanding the relative stability of key structure elements will also be critical in "man-made" chemical environments (e.g., the examples given at the outset of this paper[19−24]). In fact, the longer members ($n \geq 8$) of the polyalanine-based peptide series studied here are helices in experiment under vacuum conditions.[28,30,56] These helices are stable *in vacuo*, even up to extreme temperatures (not expected in solution),[31,57] or after soft landing on a surface.[58]

The PES also shapes the entropy and thus the effect of the temperature T. With increasing T, the conformational entropy of the backbone will favor an unfolded state[25,38,59,60] (so-called "random coil"), while, at low T, helices may also compete with other, enthalpically more stable conformers. For instance, gas-phase ion mobility spectrometry (IMS) by Jarrold and coworkers[26] showed that the $Ac\text{-}Ala_4\text{-}Gly_7\text{-}Ala_4H^+$ polypeptide is helical at T = 400 K but globular at room temperature. A similar structural change was observed in experiments involving multiply protonated polyalanine peptides in the gas-phase in ref 61. Empirical force-field-based simulations by Ma and coworkers[62] of more than 60 small peptides indicate that the *vibrational* entropy (harmonic approximation) could stabilize α-helices or β-hairpins over fully relaxed conformer ensembles obtained with random structures generated from high T trajectories, that is, attempting to mimic the "unfolded structure." A gain in vibrational entropy due to the existence of low-frequency vibrations stemming from helical and β-sheet motifs in biomolecules has also been studied with empirical theoretical models by Chou and coworkers.[63] Recently, Plowright and coworkers[64] used DFT including dispersion contributions (the B97-D[65] exchange-correlation functional) to suggest that, for a small neutral four-residue peptide, β-sheets and conformers containing 3_{10} helical loops are stabilized by the harmonic vibrational entropy at finite temperatures.

In the present work, we provide independent, unambiguous, and quantitative computational evidence that the vibrational entropy acts to stabilize helical conformers with increasing temperature over more compact, enthalpically competitive structures. What is new compared with previous studies (e.g., Ma et al.[62]) is that we have access to the full low-energy conformational ensemble, encompassing thousands of conformations that compete with helical structures toward low temperature, for peptides of significant length (up to 110 atoms), based on an accurate, fully quantum-mechanical level of theory that captures all potentially relevant effects (hydrogen bond cooperativity, strain, polarizability changes, etc.) in a completely nonempirical way. We are thus able to trace the reason for the stabilization of helices to their softer low-frequency modes, in comparison with more compact, competing low-energy conformations. We show that this lowering of frequencies also persists for the anharmonic case, evidenced by the vibrational density of states (VDOS) derived from *ab initio* molecular dynamics simulations.

We focus on polyalanine-based peptides because alanine is known to have a high helix propensity both in solution[37,66] and *in vacuo*.[8] For $Ac\text{-}Ala_n\text{-}LysH^+$ (n = 4−20) in the gas phase, IMS[29] and first-principles calculations compared with experimental vibrational spectroscopy at room temperature[30] suggest a crossover from nonhelical to helical preferred conformers as a function of polyalanine chain length. For n = 5, there is a competition between different conformers, whereas the n = 10 and 15 conformers are found to be firmly in the helical range.[30] A similar globule to helix transition also occurs for sodiated polyalanine.[67] For idealized polyalanine helix models, various past first-principles studies have dissected helix-stabilizing factors,[35,36,49,68] including an analysis of the role of electrostatics, H-bond cooperativity, and vdW interactions for the stability of unsolvated polyalanine-based helices against unfolding in our own group.[31] This class of systems is thus an ideal testing ground to clarify the structural competition of nonhelical (compact) and helical conformers as a function of chain length also toward the opposite temperature limit (low temperature, folded state). In the following, we address conformational preference of $Ac\text{-}Ala_n\text{-}LysH^+$ *in vacuo* for n = 4−8, that is, the length range in which the helical preference at room temperature develops.

METHOD

We are here primarily interested in finding the lowest energy conformers of $Ac\text{-}Ala_n\text{-}LysH^+$, n = 4−8. For an accurate description of the underlying potential-energy surface, we turn to first principles, following the same conformational search strategy previously described in refs 69 and 70. The method that we employ is density functional theory with the PBE+vdW[32,27] exchange-correlation functional. The vdW dispersion correction[27] consists of a $C_6[n]/R^6$ term, where the C_6 coefficients depend on the self-consistent electron density n.

As explained in ref 69 and 70, we start searching the conformational manifold by scanning for a wide range of structure candidates using a force-field-based (OPLS-AA[71]) basin-hopping algorithm supplied with the TINKER[72] package. No geometrical constraints are enforced in these searches. We here perform the basin-hopping search within a 50 kcal/mol energy window (2 eV), using 15 torsional modes. The procedure leads to at least 10^5 conformers for each of the molecules in question. In our searches, both the Lys residue and the C-terminal COOH are considered protonated throughout, which is the known gas-phase preference when the N-terminus is capped.[28,73,74] The force-field-guided search for structure candidates has the sole goal of providing an exhaustive list of candidate structures for the second step of our search. For the force field used, this list is converged with respect to the basin-hopping parameters, as shown in the Supporting Information (SI) and in ref 70.

The second step consists of full relaxations of a wide range of low-energy force-field conformers using the PBE+vdW functional. We perform these relaxations with the all-electron, localized basis program FHI-aims.[75,76] Using "light" settings for integration grids and basis sets, we relax 1068, 1000, 800, 800, and 820 conformers for $Ac\text{-}Ala_nLysH^+$, n = 4, 5, 6, 7, 8, respectively. We then postrelax up to 50 low-energy structures using the FHI-aims numerical "tight" settings and "tier 2" basis set, which provide essentially converged energy hierarchies free from basis-set superposition error.[75,69] All energy gradients

dx.doi.org/10.1021/jp402087e | J. Phys. Chem. B 2013, 117, 5574−5584

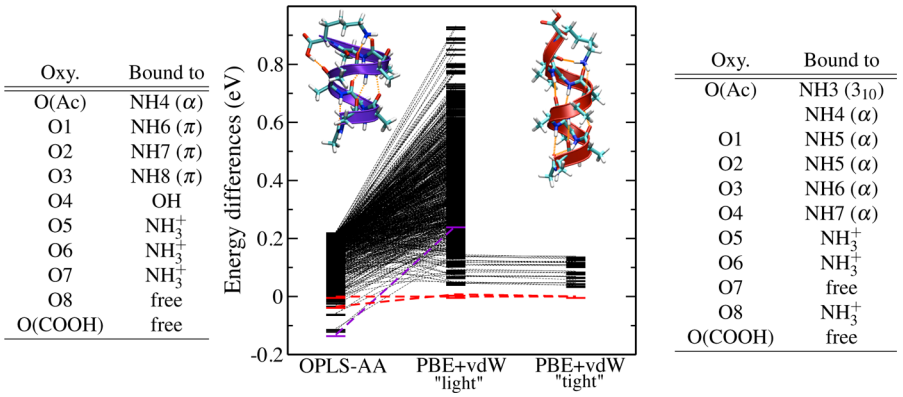

Figure 1. Center: Energy hierarchies obtained for Ac-Ala_8-$LysH^+$ with the OPLS-AA force field, PBE+vdW with "light"[75] computational settings, and PBE+vdW with "tight"[75] computational settings. All conformers are fully relaxed at each level of theory. Highlighted in red are two slightly different force-field conformers that relax to the lowest energy Family 1 (α-helical) conformer in the PBE+vdW functional. Highlighted in violet is the lowest energy OPLS-AA conformer. Left: H-bond patterns of the force-field minimum-energy conformer. Right: H-bond patterns of the PBE+vdW minimum-energy conformer.

were converged to magnitudes $<10^{-3}$ eV/Å in the final relaxed structures.

To illustrate how the conformer energy hierarchies change between the OPLS-AA force field and the PBE+vdW functional, in Figure 1, we show the OPLS-AA and PBE +vdW energetic hierarchies of all conformers relaxed with the PBE+vdW functional for Ac-Ala_8-$LysH^+$. There is a considerable energy rearrangement between the OPLS-AA force field and the PBE+vdW functional ("light" settings, "tier 1" basis set), which has also been observed for other peptides.[69,77] Importantly, the OPLS-AA force field predicts a different global minimum structure from the one predicted with the PBE+vdW functional. While the PBE+vdW functional correctly[29] predicts the α-helix as the minimum energy structure, the OPLS-AA force field predicts a mostly π-helical structure. Also shown in Figure 1 is the low-energy conformational energy hierarchy calculated with the PBE+vdW functional and FHI-aims "tight" settings. The energy hierarchy of the conformers changes by maximally 20 meV between "light" and "tight" settings. Although the energy hierarchy can strongly vary between the force field and the PBE+vdW functional, for Lys-terminated polyalanine, our experience is[69,70] that the lowest energy PBE +vdW conformer is found among the first few hundred relaxations of low-energy force-field conformers. We also note that force fields may be prone to structure-specific errors. For example, we observe that OPLS-AA systematically overestimates the energy of 3_{10}-helical structures *in vacuo*. To exclude any unwanted impact of the energetic overestimation of 3_{10}-helices, we performed additional constrained basin-hopping searches for all n, in which we constrain the central H bonds of the molecules to remain 3_{10}-helical (see Figure S1 of the SI), followed by individual, unconstrained PBE+vdW relaxations. For n = 5, we also tested the influence of other DFT functionals, reported in Figure S2 of the SI. Differences of 50 meV (<10 meV per residue) in the energy hierarchy can arise as a result of changing the functional, but as long as the vdW correction is included, the overall energy hierarchy trends are kept.

The PBE+vdW relaxed ("light" settings) conformers were sorted into "families" according to their H-bond pattern. We define a H bond to be present when an O acceptor atom is closer than 2.5 Å to a H donor atom. Within each H-bond family thus defined, small conformational variations are still possible, for example, by slight bends of the backbone atoms or different rotamers of the $LysH^+$ side chain. Typically, the lowest-energy PBE+vdW conformer is found among the family members arising within 5 kcal/mol (~0.2 eV) of the lowest-energy force-field conformer.

The PBE+vdW structure optimizations are followed by harmonic vibrational and (rigid-body) rotational free-energy calculations for the lowest-energy conformers of the H-bond families lying within 0.12 eV (~3 kcal/mol) of the global energy minimum for each n. The harmonic vibrational frequencies and intensities were also computed in FHI-aims using a finite difference approach. Our primary conclusions regarding free-energy differences in this article are based on the lowest-frequency vibrations of our conformers. To demonstrate that these modes are accurately converged in our finite-difference approach, Figure 2 shows the differences in predicted

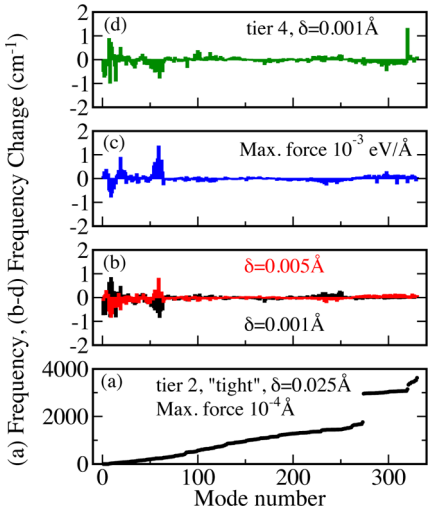

Figure 2. Numerical convergence of the finite-difference-based computed frequencies reported in this paper. (a) Vibrational frequencies of Family 1 of n = 8 (110 atoms, α-helix) in cm^{-1} against the vibrational mode number. (b–d) Numerical changes of frequencies that arise when varying: (b) the atom displacement for calculation of finite differences δ, (c) the force relaxation threshold "max. force", and (d) and the size of the basis set, "tier". The reference is taken as δ = 0.0025 Å, max. force 10^{-4} eV/Å, and tier 2 basis set.

dx.doi.org/10.1021/jp402087e | J. Phys. Chem. B 2013, 117, 5574–5584

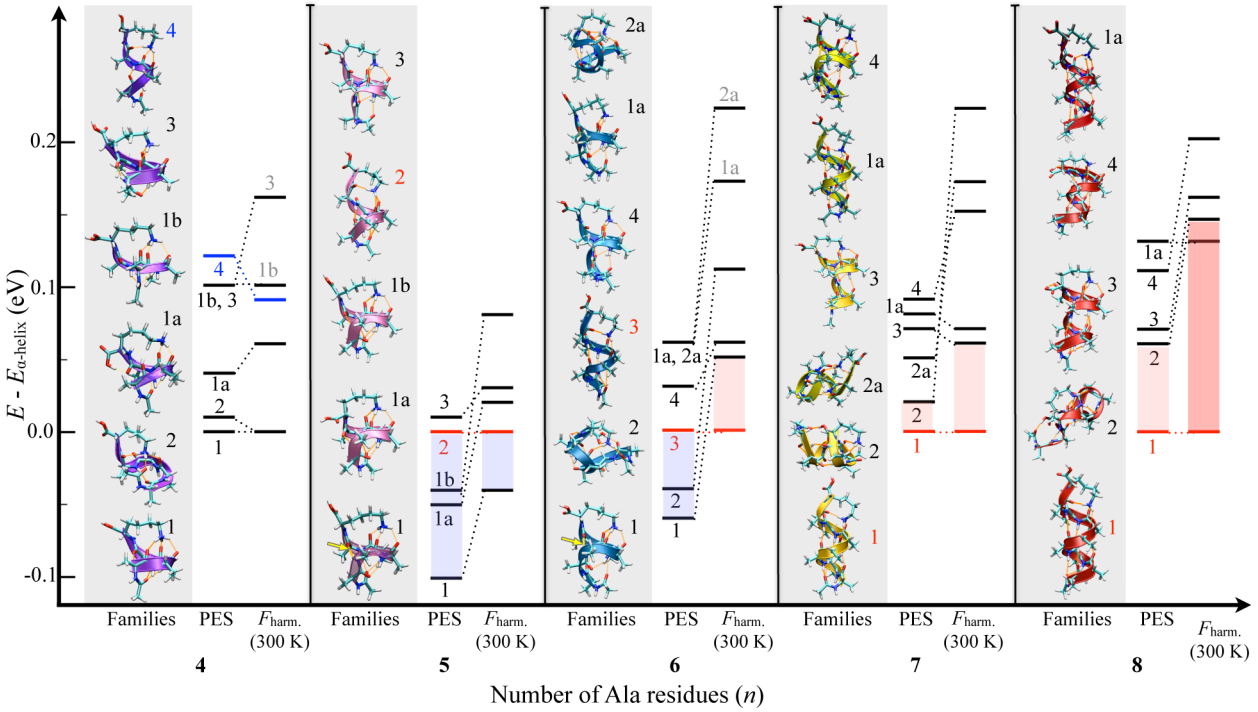

Figure 3. Energy hierarchies (thick horizontal bars), obtained with the PBE+vdW functional, for the low-energy H-bond families of Ac-Ala$_n$-LysH$^+$, n = 4−8. The "inverted" H bonds of n = 5 and 6 are highlighted in yellow and pointed to by an arrow (see text). For each n, we include the conformer representatives of the lowest-energy families up to 0.12 eV from the global minimum, as defined by local minima of the PBE+vdW potential energy surface (PES). We also show their hierarchy after adding the corrections for the harmonic vibrational free energy $F_{harm.}$ at T = 300 K. Numbers labeling each family, as well as colored structural representations are shown. The placement of the structure pictures in the shaded gray areas is not directly related to the energy axis (y axis), which applies strictly only to the horizontal bars. For these, the α-helical conformer of $n \geq 5$ is chosen as the reference (zero) energy. For n = 4, Family 1 is taken as the reference. α-Helical conformers are highlighted by red bars. The 3_{10}-helical conformer for n = 4 is highlighted by blue bars. The shaded areas in the energy hierarchies indicate the energy difference between the α-helix and the nearest nonhelical conformers.

frequencies when varying three important numerical choices: the finite-difference displacement length δ (subfigure b), the force convergence criterion used in the relaxation (subfigure c), and the quantum mechanical basis set (subfigure d). Varying our default choices (δ = 0.0025 Å, energy gradients below 10^{-3} eV/Å, and tier 2 basis set) produces frequency changes below 2 cm^{-1} at most.

For n = 8, we have also calculated vibrational densities of state beyond the harmonic approximation, taking the Fourier transform of the velocity time autocorrelation function. The trajectories were evaluated with Born−Oppenheimer *ab initio* molecular dynamics, using the PBE+vdW functional. We used a 1 fs time step, and the microcanonical simulations were 21 ps long, with FHI-aims "tight" numerical settings and "tier 2" basis set. The molecules were initially thermalized to approximately room temperature for 5 ps using the Bussi−Donadio−Parrinello[78] thermostat.

For all molecules containing n > 8 alanine residues and for the Li$^+$-terminated model structures discussed in this work, no extensive conformational search was performed. These peptides are structure models used specifically for a computer experiment to determine the development of low-frequency vibrational modes with increasing helix length for two different terminations. Their geometries are fully relaxed PBE+vdW structures, using "tight" settings and the tier 2 basis sets.

RESULTS AND DISCUSSION

Conformational Energy Hierarchy. Figure 3 summarizes the energetic ordering of the lowest-energy (PBE+vdW) H-bond families for n = 4−8 found in the present work. Only the energy of the lowest energy structure belonging to each family is reported, and families are included up to 0.12 eV (~3 kcal/mol) of the lowest identified minimum of the PBE+vdW PES. α-Helical conformers are highlighted in red. The 3_{10}-helical conformer for n = 4 is highlighted in blue. We define purely α- (or purely 3_{10}-) helical conformers as those where, counting from the N-terminus, all of the backbone CO groups at residues i are either connected to NH groups at residues i+4 (or i+3) or connected to the LysH$^+$ side chain (usually the final three or four CO groups at the C terminus). Coordinates and a more detailed analysis of all the geometries shown in Figure 3 are given in the SI.

The conformer associated with the lowest-energy PES minimum for n = 4 is rather small, connecting almost all of its backbone CO groups to the LysH$^+$ termination. The remaining H bond at the N-terminus is bifurcated; that is, the oxygen atom is involved into both an α- and a 3_{10}-helical H bond. This conformer could therefore be classified as the smallest possible α-helical prototype in this series. In contrast, the structures that correspond to the lowest-energy PES minima for n = 5 and 6 are *not* simple helices. Each contains an "inverted" H bond where one CO group points to the N-terminus and its connecting NH group points to the C-terminus, producing more compact structures. In Figure 3,

dx.doi.org/10.1021/jp402087e | J. Phys. Chem. B 2013, 117, 5574−5584

these bonds are highlighted in yellow and pointed to by an arrow. For n = 5, we have previously denoted this conformer as "g-1".[30] For n = 7 and 8, the lowest-energy PES minima correspond to α-helices. In each case, they are closely followed by a conformer that we characterize as compact/globular (Families 2 of n = 7 and 8, with an energy separation of 20 and 60 meV, respectively). Thus, we already observe a crossover with peptide length to α-helical lowest-energy minima of the PES at n = 7. However, on the basis of the energy hierarchies of the structures of the local PBE+vdW PES minima alone, one would not expect a purely helical ensemble of conformers at room temperature at n = 7 or 8. Simple Boltzmann factors would indicate a mix of structure candidates, yet the experimental work by Kohtani and Jarrold[29] does suggest a complete room-temperature structural crossover at n = 8 at the latest, albeit based on a completely different line of reasoning (water adsorption behavior of "helical" versus "globular" conformers).

For the low-energy conformers in Figure 3, we also compute and show in the same Figure the impact of the vibrational free energy at room temperature (T = 300 K) in the harmonic approximation. Differences in the free energy contributions from rigid body rotations between different conformers were evaluated to be of maximally 8 meV. Remarkably, the relative stability of the α-helices is systematically enhanced by the vibrational free energy contribution for *all n*. For n = 5 and 6, the α-helical conformers move down in energy with respect to the (nonhelical) lowest energy PES minimum. For n = 7 and 8, the α-helices now become the isolated minima. In detail, we observe:

- For n = 8, the energy interval between the α-helical lowest energy conformer and the nearest globular one (red shaded areas) now amounts to 0.14 eV. The additional Family 1a at 0.13 eV is another α-helix with a slightly modified terminating H-bond network. With the vibrational free energy included, the energy hierarchy is thus consistent with the experimental claim that α-helices dominate over all other possible conformers in gas-phase experiments for n = 8.[29,58]
- For n = 7, the same qualitative picture emerges. Here the next remaining conformer (Family 3) at 300 K is a mixed $3_{10}/\alpha$-helix. The competing compact conformers (representatives of Family 2 and 2a) are significantly destabilized by $F_{\mathrm{harm.}}(T)$.
- For n = 6, the α-helix emerges as the room-temperature minimum free-energy conformer, but the competing nonhelical PES minimum, Family 1, remains close in energy (50 meV).
- For n = 5, the difference between the α-helix and Family 1 (g-1) decreases by 60 meV at 300 K, compared with the PES minimum, but Family 1 remains overall more favorable.

In essence, there is an uniform stabilization of helical over more compact (globular) structures as the temperature increases. The stabilization tendency increases with peptide length, confirming quantitatively and systematically from first principles the related observations in refs 26, 62, and 64.

We next demonstrate that it is indeed the *vibrational entropy* term that is critical and then pinpoint the physical reason among the low-frequency vibrational modes.

Origin of the Entropic Stabilization. In Figure 4, we analyze the individual quantities composing the vibrational free-

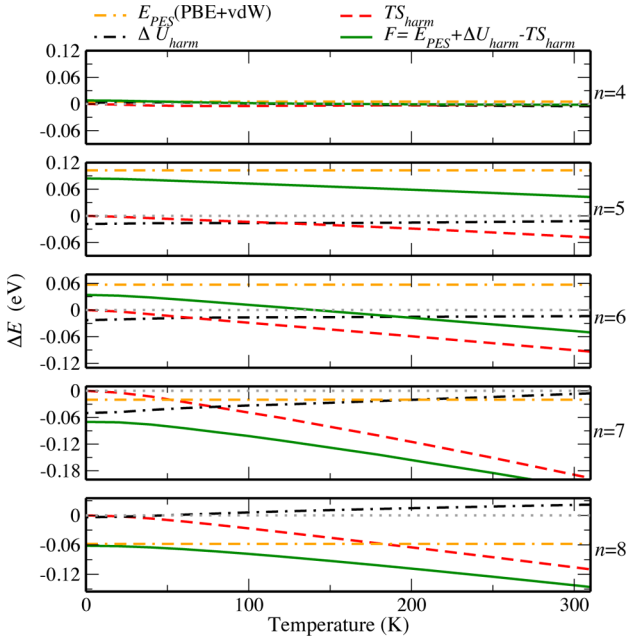

Figure 4. Energy differences for each term of the harmonic free energy as a function of temperature for: Families 1 and 2 of n = 4; Families 1 (nonhelical) and 2 (α-helical) of n = 5; Families 1 (nonhelical) and 3 (α-helical) of n = 6; Families 1 (α-helical) and 2 (compact) of n = 7; and Families 1 (α-helical) and 2 (compact) of n = 8. In each case, the non-α-helical conformer was taken as the reference (i.e., negative slopes mean α-helix stabilization). The PBE+vdW energy differences are plotted with a yellow dashed-dashed-dotted line, the harmonic internal energy $\Delta U_{\mathrm{harm.}}$ with black dashed-dotted lines, the entropy term $TS_{\mathrm{harm.}}$ with red dashed lines, and the sum $F_{\mathrm{harm.}}$ with green full lines.

energy differences between: Families 1 and 2 of n = 4, Families 1 (nonhelical) and 2 (α-helical) of n = 5, Families 1 (nonhelical) and 3 (α-helical) of n = 6, as well as Families 1 (α-helical) and 2 (compact) for n = 7 and 8. The energy terms plotted are the PBE+vdW PES minimum energy, the harmonic internal energy (containing the zero-point energy) $\Delta U_{\mathrm{harm.}}(T)$, and the entropy term $TS_{\mathrm{harm.}}(T)$. They are reported in Figure 4 as energy differences, taking the nonhelical conformer of each n as the reference, such that negative slopes correspond to a stabilization of the α-helices. Upon inspection of Figure 4, we observe a monotonic stabilization of all helical conformers with increasing T. Whereas for the shortest molecule (n = 4) there is hardly any observable effect, the stabilization trend is enhanced with increasing length. For n = 6, we predict a crossover of the lowest-energy structures at $T \approx 150$ K. It is clear that among the individual contributions to the vibrational part of the free energy $F_{\mathrm{harm.}}(T)$ the entropy term $TS_{\mathrm{harm}}(T)$ is indeed always the most important helix-favoring term. The zero-point energy (ΔU_{harm} at T = 0) also favors the helices but on a smaller energy scale.

The contribution of each mode to the helix stabilization free energy at room T can be quantified by calculating the single-mode temperature-dependent contribution to the vibrational free energy $Q_i = k_B T \ln\{1-\exp[-\hbar\omega_i/(k_B T)]\}$, where ω_i are the vibrational frequencies. The quantity that enters the computation of ΔF between different conformers here presented is the difference $\Delta Q_{\mathrm{total}} = \sum_i \Delta Q_i$. To analyze the contribution of each vibrational mode i in free energy differences, it is thus convenient to plot $\Delta Q_i/\Delta Q_{\mathrm{total}}$, the sum of which over all

dx.doi.org/10.1021/jp402087e | J. Phys. Chem. B 2013, 117, 5574−5584

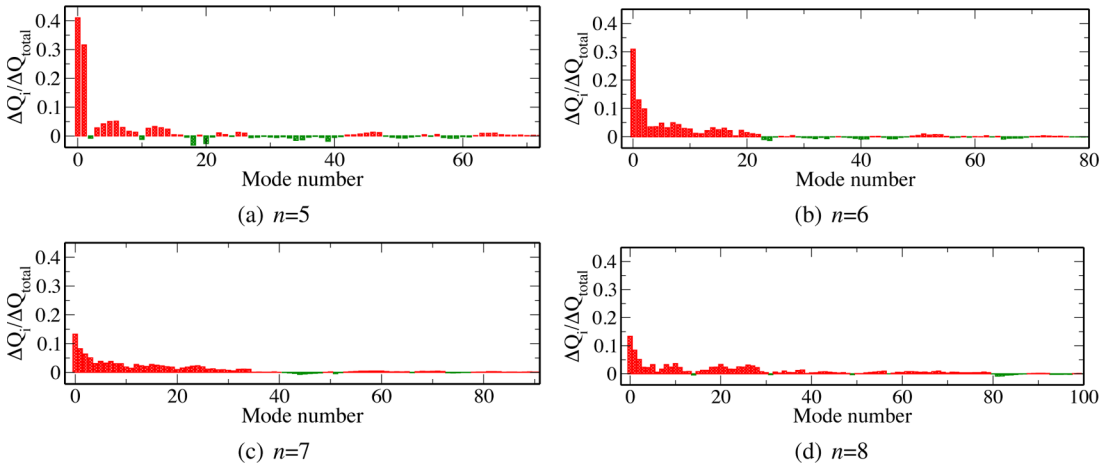

Figure 5. Contribution from single vibrational modes to the helix stabilization free energy at room temperature for the same conformers treated in Figure 4 for each n. The definition of the quantities plotted is $Q_i = k_B T \ln\{1-\exp[-\hbar\omega_i/(k_B T)]\}$, and $Q_{total} = \sum_i Q_i$. The differences Δ shown are between the α-helical conformer of each n and the nonhelical or compact conformer at each n. Positive red bars denote a contribution to α-helix stabilization with respect to the nonhelical, compact conformers, and green negative bars denote a contribution to destabilization. For all n, the wavenumber corresponding to the highest mode number plotted is ~570 cm^{-1}.

modes is normalized to one. These mode-dependent contributions are shown in Figure 5 for n = 5−8 and for the same conformers (helical vs nonhelical) included in Figure 4. The included modes i are plotted up to ~570 cm^{-1} for each n. Modes in this frequency range dominate the temperature-dependent contribution to the harmonic free energies, such that conformers with softer low-energy vibrational modes will be effectively stabilized against those that have stiffer low-energy vibrations. In Figure 5, positive bars correspond to softer modes in the α-helical conformer and thus a contribution to α-helical stabilization. We observe that the low-frequency modes contribute uniformly and overwhelmingly to the observed stabilization, reflecting the fact that α-helices have overall softer vibrational modes than compact conformers. The stabilization contribution "delocalizes" over higher energy modes as the length of the molecules is increased. The maximum frequency shown in all plots of Figure 5 is approximately the same for all n. The same qualitative conclusions hold for other functionals as well, as we exemplify in Figure S3 of the SI for the BLYP[79]+vdW functional and n = 8.

For the PBE+vdW functional, Figure 5 suggests that the very lowest-frequency vibrational modes can be taken as an indicator of the observed helical stabilization with respect to more compact conformers. Table 1 shows the frequencies (in cm^{-1}) corresponding to the first normal modes of all conformers shown in Figure 3 of the manuscript, as obtained with the PBE+vdW functional. The lowest-energy α-helices, marked in red in Table 1, show first vibrational normal modes between 8 and 13 cm^{-1}. The same is true for families 1a of n = 7 and 8, which only differ in details of the termination. In contrast, the conformers that have first vibrational modes of at least 20 cm^{-1} are all compact and nonhelical, for example: 28 cm^{-1} for Family 2 of n = 7 and 22 cm^{-1} for Family 1 (g-1 motif) of n = 5. The g-1 motif has the first vibrational mode lying around 20 cm^{-1} for n = 5, 6, and 7 (marked with a * symbol in Table 1).

Here a comment regarding structures that are more elongated than α-helices is in order. It is customary to compare the stability of α-helices with 3_{10}-helices and β-sheets or fully extended structures (FESs) (e.g., in refs 35,36,80−86 and many others). Following our rationale above, the more extended the structure is, the softer the low vibrational modes will be. This indeed happens for the most extreme case, the FES, where we find the first vibrational mode to lie around only 2 cm^{-1} (calculated for n = 8 and 15). In fact, entropically stabilized β-sheets in *neutral* polyalanine in the gas-phase have been suggested in ref 44. For 3_{10}-helices, in our own structure searches for n = 4−8, we always find the first vibrational mode to lie very close to their α-helical counterpart. Accordingly, it is the enthalpic energy difference that favors α-helices specifically over 3_{10} for all molecules studied. For infinite periodic structures, calculations of phonons and vibrational free energies for α-, 3_{10}-, and π-helices and the FES in ref 80 corroborate our results. There, all helices are destabilized with respect to the FES at 300 K. The π-helix, which is the most compact among the helices studied in ref 80, is most destabilized by the vibrational entropy term.

Table 1. Position of the Lowest Vibrational Mode in cm^{-1} and Calculated with the PBE+vdW Functional, For the Lowest Energy Conformer of Each Family Shown in Figure 3 for n = 4−8[a]

conformer/length	4	5	6	7	8
Family 1	23	22*	20*	12	11
Family 1a	27	23	21	10	11
Family 1b	25	26			
Family 2	17	13	20	28	20
Family 2a			23	22	
Family 3	27*	20	8	15	16
Family 4	17		18	20*	15

[a]We use red characters to indicate the α-helical conformers, a * symbol for the g-1-like conformers of n = 5 and 6, and blue characters for the 3_{10}-helical conformer.

Beyond the Harmonic Approximation: *Ab Initio* Molecular Dynamics. We next show that the observations discussed in the last section should hold also in a fully anharmonic picture. Even at relatively low temperature, where the overall structure is kept, we expect first the inherent anharmonicity of the local, nearly harmonic PES, then the lowest-barrier transitions between basins (side-chain rotations), and then transitions between locally different backbone conformations and H-bond networks[87,88] to contribute.

dx.doi.org/10.1021/jp402087e | J. Phys. Chem. B 2013, 117, 5574−5584

Unfortunately, a direct calculation of these terms (e.g., by thermodynamic integration) is computationally prohibitive in DFT. We can, however, use explicit *ab initio* molecular dynamics simulations to gain some insight. In Figure 6, we compare the Fourier-transformed velocity autocorrelation functions of the Family 1 (helical) and Family 2 (compact nonhelical) conformers of n = 8, extracted from explicit microcanonical *ab initio* molecular dynamics simulations (21 ps total time, 1 fs time step, initially thermalized to approximately room temperature). The Fourier transform of the velocity autocorrelation function corresponds to a VDOS. At T = 0, the VDOS should, in the approximation of classical nuclei, reflect the harmonic vibrational modes, also shown in Figure 6. Compared with these modes, the onset of the calculated VDOS at $T \approx 300$ K is noticeably shifted toward lower frequencies for both conformers, but the onset frequency for the helix is still significantly lower than that for the nonhelical structure. Thus, the lower vibrational frequencies of the helix are also carried over to the full (anharmonic) motion of the conformers. In addition, the integral over the VDOS up to 50 cm^{-1} is 6% larger for the α-helical Family 1 than for the compact Family 2; that is, the general downshift of frequencies in this region is also preserved.

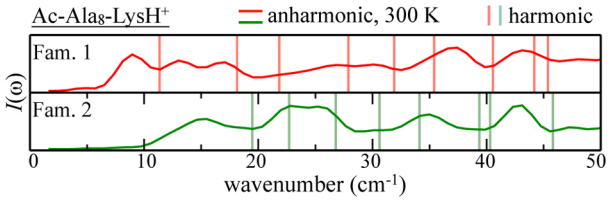

Figure 6. Vibrational density of states calculated as the Fourier transform of the velocity autocorrelation function of 21 ps long microcanonical AIMD simulations at $\langle T \rangle$ = 300 K for Family 1 (α-helix) and Family 2 (compact) of Ac-Ala_8-$LysH^+$. Light colored bars correspond to the harmonic normal frequencies of vibration for the respective conformers.

Regarding the local structural stability during the AIMD simulation, we can analyze the detailed evolution of the H-bond network of the molecules, which we show here in Figure 7a,b. The colored bars in those Figures show whether a specific kind of H bond is present at a given time during the simulation. The oxygen atoms participating in the possible H bonds are labeled from O(Ac), belonging to the acetate group of the N-terminus, up to O8, belonging to the alanine residue closest to the C-terminus. We consider a H bond every (C)O donor−NH acceptor pair lying at a distance closer than 2.5 Å. Through this definition, it is possible to count a H bond even if the charge densities would not characterize, strictly speaking, a bond. It is more important, however, that we do not miss any possible bond, and this is guaranteed by our definition. The respective fractions of the time that *helical* bonds of a specific type exist during the simulation are shown on the right side of the plot. The sum of these fractions for a given oxygen can exceed 100% because when a bond is bifurcated we count it twice, once for each kind of H bond.

We observe that the H-bond pattern of Family 2 (compact) stays essentially the same throughout the entire simulation. In contrast, Family 1 displays local structural fluctuations in the helical part, occasionally forming short-lived 3_{10}-like H-bond connections. Similar fluctuations also occur in simulations of longer helices (e.g., Ac-Ala_{15}-$LysH^+$ in ref 30). It seems plausible that the overall greater "floppiness" of the helix compared with the more compact nonhelical H-bond network adds another favorable entropic contribution at room temperature. This direct observation that we make has been conjectured as the motive for the loss in entropy observed in α-helical formation, compared with a polyproline-II (PPII) helical structure in ref 84. According to our reasoning, the PPII structure, being less compact than the α-helices, should indeed show more fluctuations, just like α-helices do if compared with more compact conformers.

Role of the Termination. Finally, we show that, especially for the short peptides considered here, there are two independent aspects to the stabilization of helical conformers: length and termination. To isolate their role, we examine the character of the lowest-frequency modes as a function of peptide length (also for longer helices) for two different terminations. The first is the $LysH^+$-terminated series, which is the main subject of this work. We contrast this series with Li^+-terminated polyalanine helices Ala_n-Li^+, a much more rigid termination as we shall see. For the latter, we define α-helical structures for all n (fully relaxed in DFT-PBE+vdW), which are

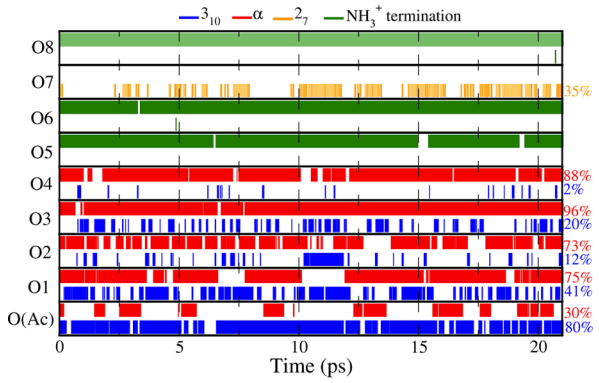

(a) Ac-Ala_8-$LysH^+$, Family 1 (helical)

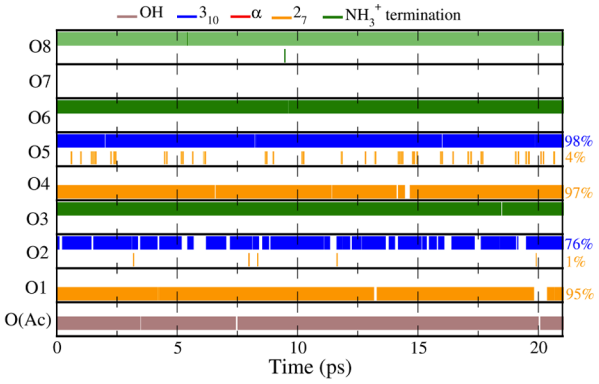

(b) Ac-Ala_8-$LysH^+$, Family 2 (compact)

Figure 7. (a) Detailed H-bond network evolution during the 21 ps long AIMD simulation (PBE+vdW, microcanonical ensemble) for the α-helical Family 1 of n = 8. (b) Detailed H-bond network evolution during the 21 ps long AIMD simulation (PBE+vdW, microcanonical ensemble) of the compact Family 2 of n = 8. Numbers shown on the right side of the plots reflect the respective fractions of time that *helical* bonds of a specific type exist during the simulation. Because a bifurcated H bond is counted twice, the overall sum for each oxygen can exceed 100%.

dx.doi.org/10.1021/jp402087e | J. Phys. Chem. B 2013, 117, 5574−5584

at least locally stable when Li^+ is placed in contact with the last three residues at the C terminus. In Figure 8a, we compare the position of the first and second vibrational modes of these α-helical geometries of Ala_n-Li^+, n = 5−15 and 20, with the α-helical geometries of Ac-Ala_n-$LysH^+$, n = 5−15 and 19. For both peptide series, there is a monotonic decrease in the first and second vibrational frequencies for $n \geq 7$, but the frequency starting point is much higher for the Li^+ termination (26 cm^{-1} at n = 7) than for the $LysH^+$ termination. A softening trend of the respective modes in neutral polyalanine helices with increasing length has also been observed in ref 89. To characterize this vibrational mode in more detail, Figure 8b visualizes the displacement of the backbone atoms of Ac-Ala_{19}-$LysH^+$ when deforming this molecule along the first vibrational mode. Figure 8c shows the relative length changes of the hydrogen bonds in the structure upon deformation along this mode. Subfigures d and e show the equivalent data for Ala_{20}-Li^+. For both molecules, the vibration spans the helical part of the structures. For the $LysH^+$-terminated molecule, we see that the actual $LysH^+$ termination (connected to the last four CO residues) is clearly involved in the vibration. In contrast, the hypothetical Li^+-charged termination constrains especially the C terminus to be much more rigid, as evidenced by the almost-zero change of all Li−O distances. Here the N-terminus is much more involved in the lowest-frequency modes. The same trends are observed for the smaller molecules in both series. Movies containing 3D visualizations of the first vibrational modes for helical and compact structures are contained in the SI. We thus conclude two points:

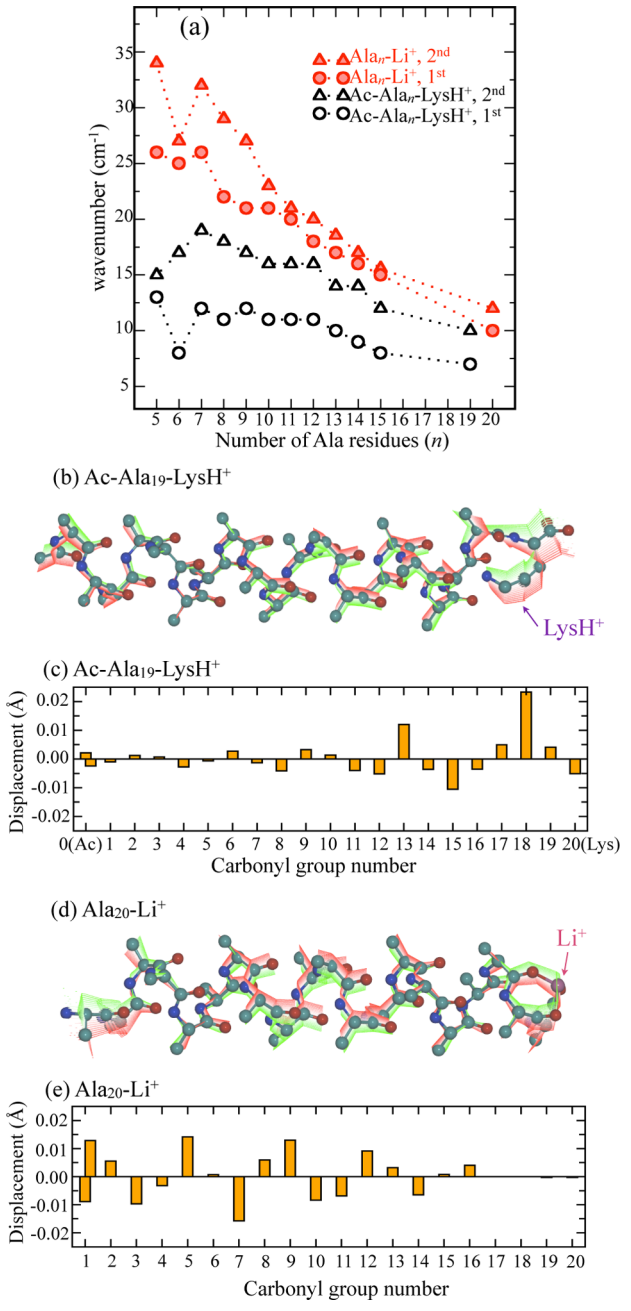

Figure 8. Characterization of the lower vibrational modes of helices considered in this work. (a) Positions of the first and second vibrational modes of α-helical geometries of Ala_n-Li^+, n = 5−15 and 20 (red) and α-helical geometries of Ac-Ala_n-$LysH^+$, n = 5−15 and 19 (black). (b) Displacement caused on the backbone atoms of Ac-Ala_{19}-$LysH^+$ by deforming this molecule in the direction of the first vibrational mode, with red shaded areas corresponding to positive displacements and green shaded areas corresponding to negative displacements (hydrogen atoms not shown). (c) Relative change in H bond distance when displacing one (normalized) unit of the first normal mode for Ac-Ala_{19}-$LysH^+$. We number the carbonyl groups from the N-terminus to the C-terminus. (d) Same as panel b for Ala_{20}-Li^+. (e) Same as panel c for Ala_{20}-Li^+. (In this case, the last three carbonyl groups do not form H bonds but are connected to the Li^+ ion.)

(i) Helices are entropically favored by allowing delocalized, soft low-frequency modes that we do not observe in competing, more compact conformers of the same $LysH^+$ termination (evidenced by Figure 5).

(ii) For short conformers, the already electrostatically favorable $LysH^+$ termination[40,43] is additionally helpful by allowing soft, delocalized modes to include the termination also for short conformers, in contrast with the hypothetical, much harder charged termination by Li^+. For long enough helices, these softer low-frequency modes should exist regardless of the termination.

CONCLUSIONS

In summary, we show from first principles, quantitatively, and for a particularly well-studied series of polyalanine peptides how helices emerge with length and temperature as the leading structural pattern from a vast array of possible competing conformers. The crossover to helical stability with length is already apparent based on local structural minima of the PES alone due to the critical role of H-bond networks including their cooperativity[31,33−36] as well as that of vdW terms.[31] In addition, the contribution from softer low-frequency vibrational modes acts to stabilize helices with increasing temperature over their more compact competition. The specific experimental claim[29] of exclusively helical conformers at and above n = 8 of Ac-Ala_n-$LysH^+$ is thus explained by *both* enthalpic and entropic effects acting together at finite temperature. *Ab initio* molecular dynamics simulations corresponding to approximately room temperature suggest that these trends are further strengthened by anharmonic effects.

The emergence of room-temperature helix stability with length in Ac-Ala_n-$LysH^+$ is thus the result of a subtle balance of enthalpic and entropic terms. In a nonvacuum environment, further terms would obviously contribute, but we expect the fact that helices, in general, allow locally softer vibrational

dx.doi.org/10.1021/jp402087e | J. Phys. Chem. B 2013, 117, 5574−5584

modes to hold. Regarding the overall ubiquity of the helical motif in folded peptides and proteins, at least, here we show that low-frequency modes will be a significant quantitative contribution.

■ ASSOCIATED CONTENT

Supporting Information

Additional computational details, the XYZ geometries of conformers discussed in this paper, detailed information (H-bond network, Ramachandran plots, relative energies) about the structures discussed in this paper, and movies illustrating the first vibrational modes of helices and compact conformers. This material is available free of charge via the Internet at http://pubs.acs.org.

■ AUTHOR INFORMATION

Corresponding Author

*E-mail: rossi@fhi-berlin.mpg.de.

Notes

The authors declare no competing financial interest.

■ ACKNOWLEDGMENTS

We acknowledge Dr. Carsten Baldauf for numerous helpful discussions and suggestions about the Figures and paper in general, including the schematic backbone vibration visualization in Figure 8.

■ REFERENCES

(1) Pauling, L.; Corey, R.; Branson, H. The Structure of Proteins: Two Hydrogen-Bonded Helical Configurations of the Polypeptide Chain. *Proc. Natl. Acad. Sci. U.S.A.* **1951**, *37*, 205−211.
(2) Berman, H. M.; et al. The Protein Data Bank. *Nucleic Acids Res.* **2000**, *28*, 235−242, http://www.pdb.org.
(3) Creighton, T. E. Stability of α-Helices. *Nature* **1987**, *326*, 547−548.
(4) Pace, N.; Scholtz, J. M. A Helix Propensity Scale Based on Experimental Studies of Peptides and Proteins. *Biophys. J.* **1998**, *75*, 422−427.
(5) Scholtz, J. M.; York, E. J.; Stewart, J. M.; Baldwin, R. L. A Neutral, Water-Soluble, A-Helical Peptide: The Effect of Ionic Strength on the Helix-Coil Equilibrium. *J. Am. Chem. Soc.* **1991**, *113*, 5102−5104.
(6) Horovitz, A.; Matthews, J. M.; Fersht, A. R. α-Helix Stability in Proteins − II. Factors That Influence Stability at an Internal Position. *J. Mol. Biol.* **1992**, *227*, 560−568.
(7) Creamer, T. P.; Rose, G. D. Side-Chain Entropy Opposes α-Helix Formation but Rationalizes Experimentally Determined Helix-Forming Propensities. *Proc. Natl. Acad. Sci. U.S.A.* **1992**, *89*, 5937−5941.
(8) Kinnear, B.; Jarrold, M. Helix Formation in Unsolvated Peptides: Side Chain Entropy Is Not the Determining Factor. *J. Am. Chem. Soc.* **2001**, *123*, 7907−7908.
(9) Miller, J.; Kennedy, R.; Kemp, D. Solubilized, Spaced Polyalanines: A Context-Free System for Determining Amino Acid A-Helix Propensities. *J. Am. Chem. Soc.* **2002**, *124*, 945−962.
(10) Scott, K. A.; Alonso, D. V.; Sato, S.; Fersht, A. R.; Daggett, V. Conformational Entropy of Alanine versus Glycine in Protein Denatured States. *Proc. Nat. Acad. Sci. U.S.A.* **2007**, *104*, 2661−2666.
(11) Moreau, R.; et al. Context-Independent, Temperature-Dependent Helical Propensities for Amino Acid Residues. *J. Am. Chem. Soc.* **2009**, *131*, 13107−13116.
(12) Barlow, D.; Thornton, J. Helix Geometry in Proteins. *J. Mol. Biol.* **1988**, *201*, 601−619.
(13) Errington, L.; Iqbalsyah, T.; Doig, A. Structure and Stability of the α-Helix. *Methods Mol. Biol.* **2006**, *340*, 3−26.
(14) Fermi, G.; Perutz, M.; Shaanan, B.; Fourme, R. The Crystal Structure of Human Deoxyhaemoglobin at 1.74 Å Resolution. *J. Mol. Biol.* **1984**, *175*, 159−174.
(15) Phillips, S. Structure and Refinement of Oxymyoglobin at 1.6 Å Resolution. *J. Mol. Biol.* **1980**, *142*, 531−554.
(16) Luger, K.; et al. Crystal Structure of the Nucleosome Core Particle at 2.8 Å Resolution. *Nature* **1997**, *389*, 251−260.
(17) Lanci, C.; et al. Computational Design of a Protein Crystal. *Proc. Natl. Acad. Sci. U.S.A.* **2012**, *109*, 7304−7309.
(18) Ma, D.; et al. Four-α-Helix Bundle with Designed Anesthetic Binding Pockets. Part I: Structural and Dynamical Analyses. *Biophys. J.* **2008**, *94*, 4454−4463.
(19) Dordick, J. S. Enzymatic Catalysis in Monophasic Organic Solvents. *Enzyme Microb. Technol.* **1989**, *11*, 194−211.
(20) Klibanov, A. M. Improving Enzymes by Using Them in Organic Solvents. *Nature* **2001**, *409*, 241−246.
(21) Laurent, N.; Haddoub, R.; Flitsch, S. L. Enzyme Catalysis on Solid Surfaces. *Enzyme Microb. Technol.* **2008**, *26*, 328−337.
(22) Swartz, J. D.; Deravi, L. F.; Wright, D. W. Bottom-Up Synthesis of Biologically Active Multilayer Films Using Inkjet-Printed Templates. *Adv. Funct. Mater.* **2010**, *20*, 1488−1492.
(23) Upert, G.; Bouillère, F.; Wennemers, H. Oligoprolines as Scaffolds for the Formation of Silver Nanoparticles in Defined Sizes: Correlating Molecular and Nanoscopic Dimensions. *Angew. Chem., Int. Ed.* **2012**, *51*, 4231−4234.
(24) Stodulski, M.; Gulder, T. Nanoparticles and Peptides: A Fruitful Liaison for Biomimetic Catalysis. *Angew. Chem., Int. Ed.* **2012**, *51*, 11202−11204.
(25) Zimm, B. H.; Bragg, J. K. Theory of the Phase Transition between Helix and Random Coil in Polypeptide Chains. *J. Chem. Phys.* **1959**, *31*, 526−535.
(26) Kinnear, B.; Hartings, M.; Jarrold, M. The Energy Landscape of Unsolvated Peptides: Helix Formation and Cold Denaturation in Ac-$A_4G_7A4^+H^+$. *J. Am. Chem. Soc.* **2002**, *124*, 4422−4431.
(27) Tkatchenko, A.; Scheffler, M. Accurate Molecular van der Waals Interactions from Ground-State Electron Density and Free-Atom Reference Data. *Phys. Rev. Lett.* **2009**, *102*, 073005.
(28) Hudgins, R. R.; Ratner, M. A.; Jarrold, M. F. Design of Helices That Are Stable in Vacuo. *J. Am. Chem. Soc.* **1998**, *120*, 12974−12975.
(29) Kohtani, M.; Jarrold, M. Water Molecule Adsorption on Short Alanine Peptides: How Short Is the Shortest Gas-Phase Alanine-Based Helix? *J. Am. Chem. Soc.* **2004**, *126*, 8454−8458.
(30) Rossi, M.; et al. Secondary Structure of Ac-Alan-LysH+ Polyalanine Peptides (n = 5,10,15) in Vacuo: Helical or Not? *J. Phys. Chem. Lett.* **2010**, *1*, 3465−3470.
(31) Tkatchenko, A.; Rossi, M.; Blum, V.; Ireta, J.; Scheffler, M. Unraveling the Stability of Polypeptide Helices: Critical Role of van der Waals Interactions. *Phys. Rev. Lett.* **2011**, *106*, 118102.
(32) Perdew, J. P.; Burke, K.; Ernzerhof, M. Generalized Gradient Approximation Made Simple. *Phys. Rev. Lett.* **1996**, *77*, 3865−3868.
(33) Guo, H.; Karplus, M. Solvent Influence on the Stability of the Peptide Hydrogen Bond: A Supramolecular Cooperative Effect. *J. Phys. Chem.* **1994**, *98*, 7104−7105.
(34) Baldwin, R. L. In Search of the Energetic Role of Peptide Hydrogen Bonds. *J. Biol. Chem.* **2003**, *278*, 17581−17588.
(35) Ireta, J.; Neugebauer, J.; Scheffler, M.; Rojo, A.; Galván, M. Density Functional Theory Study of the Cooperativity of Hydrogen Bonds in Finite and Infinite α-Helices. *J. Phys. Chem. B* **2003**, *107*, 1432−1437.
(36) Wieczorek, R.; Dannenberg, J. J. Comparison of Fully Optimized α- and 3_{10}-Helices with Extended β-Strands. An ONIOM Density Functional Theory Study. *J. Am. Chem. Soc.* **2004**, *126*, 14198−14205.
(37) Scholtz, J. M.; Baldwin, R. L. The Mechanism of α-Helix Formation by Peptides. *Annu. Rev. Biophys. Biomol. Struct.* **1992**, *21*, 95−118 and references therein.
(38) Baldwin, R. L. Energetics of Protein Folding. *J. Mol. Biol.* **2007**, *371*, 283−301.
(39) Blagdon, D. E.; Goodman, M. Mechanisms of Protein and Polypeptide Helix Initiation. *Biopolymers* **1975**, *14*, 241−245.
(40) Presta, L. G.; Rose, G. D. Helix Signals in Proteins. *Science* **1988**, *240*, 1632−1641.

(41) Serrano, L.; Fersht, A. R. Capping and α-Helix Stability. *Nature* **1989**, *342*, 296−299.
(42) Takahashi, S.; Kim, E. H.; Hibino, T.; Ooi, T. Comparison of α-Helix Stability in Peptides Having a Negatively or Positively Charged Residue Block Attached Either to the N- or C-Terminus of an α-Helix: The Electrostatic Contribution and Anisotropic Stability of The α-Helix. *Biopolymers* **1989**, *28*, 995−1009.
(43) Marqusee, S.; Robbins, V.; Baldwin, R. Unusually Stable Helix Formation in Short Alanine-Based Peptides. *Proc. Natl. Acad. Sci. U.S.A.* **1989**, *86*, 5286−5290.
(44) Dugourd, P.; Antoine, R.; Breaux, G.; Broyer, M.; Jarrold, M. Entropic Stabilization of Isolated β-Sheets. *J. Am. Chem. Soc.* **2005**, *127*, 4675−4679.
(45) Williams, L.; Kristian, K.; Kemp, D. High Helicities of Lys-Containing, Ala-Rich Peptides Are Primarily Attributable to a Large, Context Dependent Lys Stabilization. *J. Am. Chem. Soc.* **1998**, *120*, 11033−11043.
(46) Hua, S.; Xu, L.; Li, W.; Li, S. Cooperativity in Long α and 310-Helical Polyalanines: Both Electrostatic and van der Waals Interactions are Essential. *J. Phys. Chem. B* **2011**, *115*, 11462−11469.
(47) Liu, D.; Wyttenbach, T.; Bowers, M. Hydration of Protonated Primary Amines: Effects of Intermolecular and Intramolecular Hydrogen Bonds. *Int. J. Mass Spectrom.* **2004**, *236*, 81−90.
(48) Job, G. E.; et al. Temperature- and Length-Dependent Energetics of Formation for Polyalanine Helices in Water: Assignment of $w_{Ala}(n,T)$ and Temperature-Dependent CD Ellipticity Standards. *J. Am. Chem. Soc.* **2006**, *128*, 8227−8233.
(49) Elstner, M.; Jalkanen, K. J.; Knapp-Mohammady, M.; Frauenheim, T.; Suhai, S. DFT Studies on Helix Formation in N-acetyl-(-alanyl)$_n$-N-methylamide for n=1−20. *Chem. Phys.* **2000**, *256*, 15−27.
(50) Salvador, P.; Asensio, A.; Dannenberg, J. J. The Effect of Aqueous Solvation upon Alpha-Helix Formation for Polyalanines. *J. Phys. Chem. B* **2007**, *111*, 7462−7466.
(51) García, A. E.; Sanbonmatsu, K. Y. α-Helical Stabilization by Side Chain Shielding of Backbone Hydrogen Bonds. *Proc. Natl. Acad. Sci.* **2002**, *99*, 2782−2787.
(52) Tirado-Rives, J.; Maxwell, D. S.; Jorgensen, W. L. Molecular Dynamics and Monte Carlo Simulations Favor the α-Helical Form for Alanine-Based Peptides in Water. *J. Am. Chem. Soc.* **1993**, *115*, 11590−11593.
(53) Kauzmann, W. Some Factors in the Interpretation of Protein Denaturation. *Adv. Protein Chem.* **1959**, *14*, 1−63.
(54) MacKenzie, K. R.; Prestegard, J. H.; Engelman, D. M. A Transmembrane Helix Dimer: Structure and Implications. *Science* **1997**, *276*, 131−133.
(55) Khutorsky, V. A-Hairpin Stability and Folding of Transmembrane Segments. *Biochem. Biophys. Res. Commun.* **2003**, *301*, 31−34.
(56) Jarrold, M. Helices and Sheets in Vacuo. *Phys. Chem. Chem. Phys.* **2007**, *9*, 1659−1671 and references therein..
(57) Kohtani, M.; Jones, T.; Schneider, J.; Jarrold, M. Extreme Stability of an Unsolvated Alpha-Helix. *J. Am. Chem. Soc.* **2004**, *24*, 7420−7421.
(58) Hu, Q.; Wang, P.; Laskin, J. Effect of the Surface on the Secondary Structure of Soft Landed Peptide Ions. *Phys. Chem. Chem. Phys.* **2010**, *12*, 12802−12810.
(59) Brooks, C.; Karplus, M.; Pettitt, M. *Proteins: A Theoretical Perspective of Dynamics, Structure, and Thermodynamics*, 1st ed.; Advances in Chemical Physics; Wiley-VCH: New York, 1988; Vol. *71*, pp 180−183.
(60) Poulain, P.; Calvo, F.; Antoine, R.; Broyer, M.; Dugourd, Ph. Competition between Secondary Structures in Gas Phase Polyalanines. *Europhys. Lett.* **2007**, *79*, 66003.
(61) Counterman, A.; Clemmer, D. Compact → Extended Helix Transitions of Polyalanine in Vacuo. *J. Phys. Chem. B* **2003**, *107*, 2111−2117.
(62) Ma, B.; Tsai, C. J.; Nussinov, R. A Systematic Study of the Vibrational Free Energies of Polypeptides in Folded and Random States. *Biophys. J.* **2000**, *79*, 2739−2753.
(63) Chou, K.-C. Low-Frequency Collective Motion in Biomacromolecules and Its Biological Functions. *Enzyme and Microbial Technology* **1988**, *30*, 3−48.
(64) Plowright, R. J.; Gloaguen, E.; Mons, M. Compact Folding of Isolated Four-Residue Neutral Peptide Chains: H-Bonding Patterns and Entropy Effects. *ChemPhysChem* **2011**, *12*, 1889−1899.
(65) Grimme, S. Semiempirical GGA-Type Density Functional Constructed with a Long-Range Dispersion Correction. *J. Comput. Chem.* **2006**, *27*, 1787−1799.
(66) Chakrabartty, A.; Baldwin, R. L. Stability of α-Helices. *Adv. Protein Chem.* **1995**, *46*, 141−176.
(67) Martens, J.; Compagnon, I.; Nicol, E.; McMahon, T.; Clavaguéra, C.; Ohanessian, G. Globule to Helix Transition in Sodiated Polyalanines. *J. Phys. Chem. Lett.* **2012**, *3*, 3320−3324.
(68) Wieczorek, R.; Dannenberg, J. J. H-Bonding Cooperativity and Energetics of ?-Helix Formation of Five 17-Amino Acid Peptides. *J. Am. Chem. Soc.* **2003**, *125*, 8124−8129.
(69) Chutia, S.; Rossi, M.; Blum, V. Water Adsorption at Two Unsolvated Peptides with a Protonated Lysine Residue: From Self-Solvation to Solvation. *J. Phys. Chem. B* **2012**, *116*, 14788−14804.
(70) Rossi, M. *Ab Initio Study of Alanine-Based Polypeptide Secondary-Structure Motifs in the Gas Phase*, Ph.D. Thesis, Fritz-Haber-Institut der Max-Planck-Gesellschaft and Technische Universität Berlin, 2011. http://opus.kobv.de/tuberlin/volltexte/2012/3429/.
(71) Kaminski, G. A.; Friesner, R. A.; Tirado-Rives, J.; Jorgensen, W. L. Evaluation and Reparametrization of the OPLS-AA Force Field for Proteins via Comparison with Accurate Quantum Chemical Calculations on Peptides. *J. Phys. Chem. B* **2001**, *105*, 6474−6487.
(72) Ponder, J. *Tinker - Software Tools for Molecular Design*. In this work, we used versions 4.2 and 5.1 of the program and the force field versions distributed within the package.
(73) McLean, J.; et al. Factors That Influence Helical Preferences for Singly Charged Gas-Phase Peptide Ions: The Effects of Multiple Potential Charge-Carrying Sites. *J. Phys. Chem. B* **2010**, *114*, 809−816.
(74) Wieczorek, R.; Dannenberg, J. α-Helical Peptides Are Not Protonated at the N-Terminus in the Gas Phase. *J. Am. Chem. Soc.* **2004**, *126*, 12278−12279.
(75) Blum, V.; et al. Ab Initio Molecular Simulations with Numeric Atom-Centered Orbitals. *Comput. Phys. Commun.* **2009**, *180*, 2175−2196.
(76) Havu, V.; Blum, V.; Havu, P.; Scheffler, M. Efficient O(N) Integration for All-Electron Electronic Structure Calculation Using Numeric Basis Functions. *J. Comput. Phys.* **2009**, *228*, 8367−8379.
(77) Baldauf, C.; Pagel, K.; Warnke, S.; von Helden, G.; Koksch, B.; Blum, V.; Scheffler, M. How Cations Change Peptide Structure. *Chem. Eur. J.* **2013**, DOI: 10.1002/chem.201204554.
(78) Bussi, G.; Donadio, D.; Parrinello, M. Canonical Sampling through Velocity Rescaling. *J. Chem. Phys.* **2007**, *126*, 014101.
(79) (a) Lee, C.; Yang, W.; Parr, R. Development of the Colle-Salvetti Correlation-Energy Formula into a Functional of the Electron Density. *Phys. Rev. B* **1988**, *37*, 785. (b) Becke, A. Correlation Energy of an Inhomogeneous Electron Gas: A Coordinate-Space Model. *J. Chem. Phys.* **1988**, *88*, 1053.
(80) Ismer, L.; Ireta, J.; Neugebauer, J. First-Principles Free-Energy Analysis of Helix Stability: The Origin of the Low Entropy in Π Helices. *J. Phys. Chem. B* **2008**, *112*, 4109−4112.
(81) Improta, R.; Barone, V.; Kudin, K.; Scuseria, G. Structure and Conformational Behavior of Biopolymers by Density Functional Calculations Employing Periodic Boundary Conditions. I. The Case of Polyglycine, Polyalanine, and Poly-α-aminoisobutyric Acid in Vacuo. *J. Am. Chem. Soc.* **2001**, *123*, 3311−3322.
(82) Topol, I.; et al. α- and 3_{10}-Helix Interconversion: A Quantum-Chemical Study on Polyalanine Systems in the Gas Phase and in Aqueous Solvent. *J. Am. Chem. Soc.* **2001**, *123*, 6054−6060.

(83) Wu, Y.-D.; Zhao, Y.-L. A Theoretical Study on the Origin of Cooperativity in the Formation of 3_{10}- and α-Helices. *J. Am. Chem. Soc.* **2001**, *123*, 5313−5319.
(84) Shi, Z.; Olson, C.; Rose, G.; Baldwin, R.; Kallenbach, N. Polyproline II Structure in a Sequence of Seven Alanine Residues. *Proc. Natl. Acad. Sci. U.S.A.* **2002**, *99*, 9190−9195.
(85) Bour, P.; Kubelka, J.; Keiderling, T. Ab Initio Quantum Mechanical Models of Peptide Helices and Their Vibrational Spectra. *Biopolymers* **2002**, *65*, 45−59.
(86) Penev, E.; Ireta, J.; Shea, J.-E. Energetics of Infinite Homopolypeptide Chains: A New Look at Commonly Used Force Fields. *J. Phys. Chem. B* **2008**, *112*, 6872−6877.
(87) Tournier, A. L.; Smith, J. C. Principal Components of the Protein Dynamical Transition. *Phys. Rev. Lett.* **2003**, *91*, 208106.
(88) Hong, L.; Smolin, N.; Lindner, B.; Sokolov, A. P.; Smith, J. C. Three Classes of Motion in the Dynamic Neutron-Scattering Susceptibility of a Globular Protein. *Phys. Rev. Lett.* **2011**, *107*, 148102.
(89) Itoh, K.; Ikeda, A.; Iwamoto, T.; Nishizawa, S. DFT Calculation Analysis of Terahertz Time-Domain Spectra of Polyalanines. *J. Mol. Struct.* **2011**, *1006*, 52−58.